Conversion of CO_2 in a cylindrical dielectric barrier discharge reactor: Effects of plasma processing parameters and reactor design

Danhua Mei and Xin Tu*

Department of Electrical Engineering and Electronics, University of Liverpool, Brownlow Hill, Liverpool, L69 3GJ, UK

* Corresponding author

Dr. Xin Tu

Department of Electrical Engineering and Electronics

University of Liverpool

Liverpool L69 3GJ

UK

E-mail: xin.tu@liverpool.ac.uk

Graphical abstract

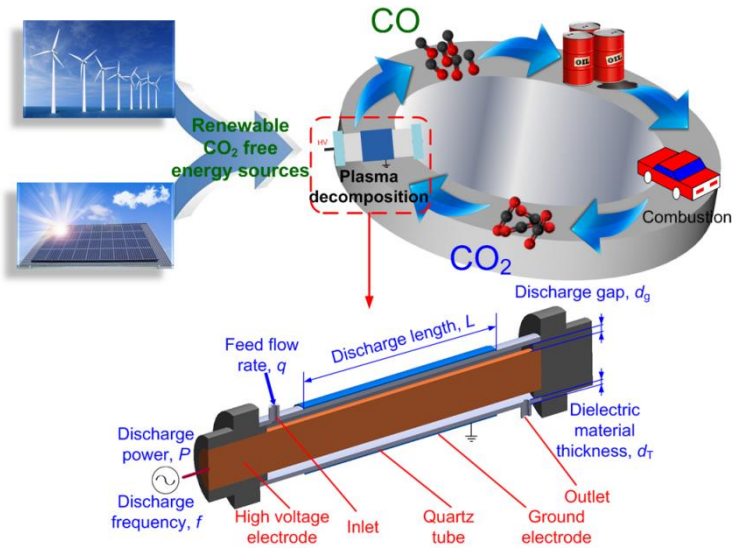

Abstract

Direct conversion of CO_2 into CO and O_2 was carried out in a cylindrical dielectric barrier discharge (DBD) reactor at atmospheric pressure and low temperatures. The influence of plasma processing parameters (e.g. discharge frequency, CO_2 flow rate, discharge power, discharge length, discharge gap, and dielectric material's thickness) on the plasma CO_2 conversion and energy efficiency of the process was investigated. The major products of this reaction were CO and O_2, which suggests the stoichiometric conversion of CO_2 into CO and O_2 was achieved. The results indicate that the frequency of discharge has a negligible influence on the conversion of CO_2 at a constant discharge power. Increasing discharge power or decreasing feed flow rate enhanced CO_2 conversion but lowered the energy efficiency when keeping other parameters constant. In addition, decreasing discharge gap and dielectric material's thickness, or enlarging discharge length can increase both the conversion of CO_2 and process efficiency. Two regression models for the plasma process were developed to elucidate the relative significance of these plasma processing parameters on the plasma conversion of CO_2. It is found that the flow rate of CO_2 and discharge power play the most important role in CO_2 conversion, while the energy efficiency is most significantly influenced by the discharge power. Modification of the plasma design was explored by using different inner electrodes and outer electrodes in the DBD system. The combination of the Al foil outer electrode with the stainless steel (SS) screw-type inner electrode showed the enhanced CO_2 conversion and energy efficiency compared to other electrode forms, leading to the maximum CO_2 conversion of 27.2% and maximum energy efficiency of 10.4% in this work. The use of the SS screw-type inner electrode could initiate enhanced local electric field near the sharp edge of the electrode, while the use of Al foil as an outer electrode could enlarge the effectiveness of discharge area compared to the mesh electrode. Both effects contributed to the enhanced efficiency of the plasma CO_2 conversion.

Keywords: non-thermal plasma; dielectric barrier discharge; CO_2 conversion; energy efficiency; reactor design

1. Introduction

The increase of energy demand in the modern society has significantly increased the consumption of carbon-containing fossil fuels on an unprecedented scale, which unfortunately releases a large amount carbon dioxide into the atmosphere. CO_2 has been considered as the main contributor to greenhouse gas effect and global warming. The concentration of CO_2 in the atmosphere increased to ~ 400 ppm in 2013, which is 42% more than that of preindustrial level [1]. The growing CO_2 concentration has caused catastrophic effect to the ecosystem, including the increase of surface temperature and sea-level, the change of hydrological and vegetation patterns, and the occurrence of disastrous weather. From this perspective, it is of primary importance to reduce the emission of CO_2, especially from anthropogenic sources. To limit global temperature rise to less than 2.0 ^oC, the worldwide CO_2 emission must has a reduction of 40-70% by 2050 versus that of 2010 [2]. The UK government has committed to reduce CO_2 emission by at least 80% by 2050 from the 1990 level [3].

Carbon capture and storage (CCS) was proposed to reduce CO_2 emission from human activities. It involves carbon capturing from industrial processes, injection and storage in different forms (e.g. geological, ocean and mineral storages) [4]. Although CCS is considered technically feasible, it is not a permanent solution to the carbon emission due to the high cost, the low public acceptance and the risk of leakage during or after injection [5]. Therefore, it is urgent to develop other sustainable alternatives which have little or no environmental impacts and zero CO_2 emissions. Carbon capture and utilization (CCU) is a promising approach to sustainably reduce carbon emissions. Rather than being treated as a waste, the captured and separated CO_2 from industrial processes can be used a feedstock to produce value-added chemicals and fuels (e.g. CO, CH_4, methanol, and DME) [6, 7]. In recent years, different technologies have been proposed for the conversion of CO_2 into valuable chemicals and fuels, including thermochemical conversion [8], electrochemical conversion [9], and photochemical conversion [10]. Among them, direct conversion of CO_2 to CO and O_2 (Eq.1) has gained significant attention as CO is a very important chemical feedstock for the synthesis of organic acid, aldehydes and alcohols [11]. Moreover, CO is also a critical C_1 feedstock for the Fischer-Tropsch process which delivers liquid hydrocarbons, synthetic petroleum and oxygenates [12].

However, CO_2 is a stable and inert molecule and it is a great challenge to convert CO_2 energy efficiently and cost-effectively. Significant amount of energy is required to overcome thermodynamic barrier for CO_2 activation. Previous thermodynamic equilibrium calculation reported that a very high temperature (3000-3500 K) is required for the reasonable conversion of CO_2 (~ 60%), which will definitely incur high energy cost in thermal decomposition of CO_2 [13].

$$CO_2 \rightarrow CO + \frac{1}{2}O_2 \qquad \Delta H = 280\,\mathrm{kJ/mol} \tag{1}$$

Non-thermal plasma (NTP) technology offers a promising and attractive alternative solution to the effective conversion of CO_2 into valuable chemicals and fuels. The gas kinetic temperature in non-thermal plasmas can be as low as room temperature, while the produced energetic electrons have high electron temperatures (1-10 eV), which can activate inert molecules (e.g. CO_2) and produce a cascade of reactive species (e.g. free radicals, excited atoms, ions and molecules) for chemical reactions [14]. This non-equilibrium characteristic enables thermodynamically unfavourable reactions to occur at low temperatures. In this regard, non-thermal plasma has been used for the synthesis of fuels and chemicals [14-25]. In addition, the compactness and flexibility (instant start-up and switch off) of non-thermal plasma processes provides great potential to integrate with renewable energy sources (e.g. solar and wind energy) and serve as a potential chemical energy storage for the surplus electricity from renewable energy during the peak moment on the grid [26]. The integrated process could in turn create a carbon-neutral network. Various NTP systems have been proposed for the direct conversion of CO_2, including dielectric barrier discharge (DBD) [13, 27-46], gliding arc discharge [47-49], corona discharge [50, 51], microwave discharge [52, 53] and glow discharge [54, 55]. The use of DBD for the conversion and utilization of CO_2 has attracted significant interest due to the following advantages: (i) A DBD plasma system has a simple structure and can be scaled up for industrial applications, which have been demonstrated in ozone production and gas clean-up [56]; (ii) Catalysts can be combined with a DBD plasma to generate a hybrid plasma-catalytic process, which has great potential to produce a synergy, thereby enhancing the conversion of CO_2, the yield and selectivity of target products and energy efficiency of the process. This has been demonstrated in the plasma-catalytic processes for energy production and gas cleaning processes using DBD plasmas [14, 57-59].

The performance of plasma CO_2 conversion using DBD plasmas is strongly related to a range of plasma processing parameters (e.g. frequency, discharge power, dielectric materials, and feed flow rate) [27, 30, 31, 35-37]. However, most of previous works were concentrated on the investigation of a few plasma processing parameters (e.g. 1-4 parameters) on the conversion of CO_2 rather than the exploration of a wide range of operating parameters used in a DBD reactor. In addition, the relative significance of these plasma processing parameters on the plasma conversion of CO_2 is also not clear [35], which is key for the optimization of the plasma processing of CO_2. One of the major challenges in the use of plasma for CO_2 conversion is how to further enhance the energy efficiency of plasma process and make this process more competitive and attractive. The combination of DBD with suitable catalysts could be one promising option to achieve this objective. However, it is difficult to find cost-effective and highly active catalysts for the plasma-catalytic processing of CO_2 into CO and O_2. Modification of DBD plasma reactor or developing new design concept might open a new route to enhance the energy efficiency of plasma process for CO_2 conversion. To the best of our knowledge, very limited work has been dedicated to evaluate the effect of different reactor configurations or designs on the plasma chemical reactions especially the conversion of CO_2.

In this work, the effect of a wide range of plasma processing parameters (e.g. discharge frequency, CO_2 flow rate, discharge power, discharge length, discharge gap and dielectric material thickness) on the conversion of CO_2 and efficiency of the plasma process has been evaluated in a cylindrical DBD reactor. Regression models for CO_2 conversion and energy efficiency based on these plasma operating parameters were developed to understand the relative significance of these parameters on the plasma CO_2 conversion. To get a better understanding of the influence of the reactor design on the plasma conversion of CO_2, different types of inner electrode (stainless steel (SS) rod electrode or SS screw-type electrode) and outer electrode (SS mesh or Al foil) were used to form different reaction configurations.

2. Experimental

2.1 Experimental setup

The experiments were carried out in a cylindrical DBD reactor, as shown in Fig. 1 (a). An outer electrode was wrapped over a quartz tube with an external diameter (D_o) of 25 mm and an inner diameter (D_i) of 20-22 mm. The length of the outer electrode can be varied from 60 to 140 mm to adjust the discharge length (L). An inner electrode with an outer diameter (d_o) of 15-17 mm was placed in the center of the quartz tube. The outer electrode was connected to the ground via an external capacitor C_{ext} (0.47 μF) and the inner electrode was powered by a high voltage output. Pure CO_2 was used as the feed gas with a flow rate of 25-125 mL/min. The DBD reactor was connected to a high voltage AC power supply with a maximum peak voltage of 30 kV and a frequency of 5-20 kHz. The applied voltage (U_a) was recorded by a high voltage probe (Testec, HVP-15HF), while the current (I_t) was measured by a current monitor (Bergoz CT-E0.5). The voltage (U_c) on the external capacitor was used to determine the charge generated in the DBD. All the signals were recorded by a four-channel oscilloscope (TDS2014). A homemade control system was developed for the measurement of the discharge power via the area calculation of the Lissajous figure in real time.

To understand the influence of the reactor design on the plasma conversion of CO_2, different types of inner electrode (SS rod electrode or SS screw-type electrode) and outer electrode (SS mesh or Al foil) were used to form different reactor designs. A design with a SS rod inner electrode and a SS mesh outer electrode was used as a reference DBD reactor. The experimental conditions of the plasma reaction with different reactor configurations are listed in Table 1.

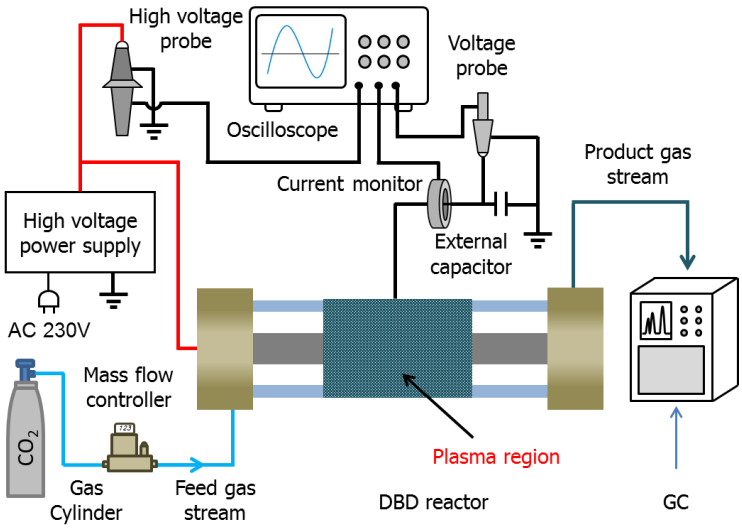

(a)

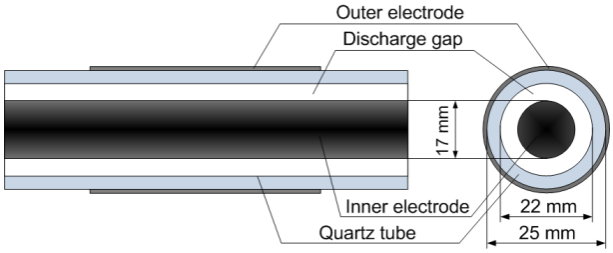

(b)

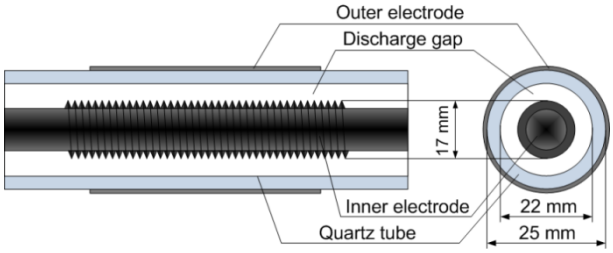

(c)

Fig. 1. Schematic diagram of the experimental system: (a) Experimental setup; (b) DBD reactor with a SS rod inner electrode; (c) DBD reactor with a SS screw-type inner electrode

Table 1 Configurations of the DBD reactor and different experimental conditions

	Discharge frequency (f, kHz)	Discharge power (P, W)	Feed flow rate (q, mL/min)	Discharge gap (d_g, mm)	Discharge length (L, mm)	Dielectric material thickness (d_T, mm)	Inner electrode	Outer electrode
Effect of f	8, 9, 10, 11	40	25	2.5	100	1.5	SS rod	SS mesh
Effect of P	9	10, 20, 30, 40, 50	25	2.5	100	1.5	SS rod	SS mesh

Effect of q	9	50	25, 31.2, 41.2, 62.5, 125	2.5	100	1.5	SS rod	SS mesh
Effect of d_g	9	10, 20, 30, 40, 50	25	2.5, 3.0, 3.5	100	1.5	SS rod	SS mesh
Effect of L	9	10, 20, 30, 40, 50	25	2.5	60, 100, 140	1.5	SS rod	SS mesh
Effect of d_T	9	10, 20, 30, 40, 50	25	2.5	100	1.5, 2.0, 2.5	SS rod	SS mesh
	9	10, 20, 30, 40, 50	25	2.5	100	1.5	SS rod	Al foil
Effect of electrode configuration	9	10, 20, 30, 40, 50	25	2.5	100	1.5	SS screw	SS mesh
	9	10, 20, 30, 40, 50	25	2.5	100	1.5	SS screw	Al foil

2.2 Gas analysis and parameter definition

The feed and gas products were analyzed by a gas chromatography (GC, Shimadzu GC2014) equipped with a thermal conductivity detector (TCD) and a flame ionization detector (FID) and. Each measurement was repeated three times when the reaction reached to a steady state. The conversion of CO_2 (C), CO selectivity (S) and carbon balance (B) are defined as follows:

$$C_{CO_2}(\%) = \frac{CO_2 \text{ converted } (\text{mol/s})}{CO_2 \text{ introduced } (\text{mol/s})} \times 100 \quad (2)$$

$$S_{CO}(\%) = \frac{CO \text{ produced } (\text{mol/s})}{CO_2 \text{ converted} (\text{mol/s})} \times 100 \quad (3)$$

$$B_{Carbon} = \frac{CO_2 \text{ output } (\text{mol/s}) + CO \text{ produced} (\text{mol/s})}{CO_2 \text{ introduced } (\text{mol/s})} \quad (4)$$

The specific energy input (SEI) and energy efficiency of the plasma process (η) are determined by

$$\text{SEI}(\text{kJ/l}) = \frac{\text{Discharge power}(\text{W})}{CO_2 \text{ flow rate}(\text{ml/s})} \quad (5)$$

$$\eta(\%) = \frac{CO_2 \text{ flow rate } (\text{ml/s}) \cdot C_{CO_2}(\%) \cdot \Delta H \, (\text{kJ/mol})}{22.4 \times \text{Discharge power } (\text{W})} \quad (6)$$

where ΔH is the reaction enthalpy (280 kJ/mol) of pure CO_2 decomposition (shown in Eq. (1)).

The transferred charge in the DBD was obtained from the Q-U Lissajous figure. The details can be found in our previous works [13, 60].

3. Results and discussions

3.1 Effect of discharge frequency

Fig. 2 shows the effect of discharge frequency on the conversion of CO_2 and energy efficiency of the plasma process. Both CO_2 conversion and energy efficiency were slightly decreased when increasing the discharge frequency from 8 to 11 kHz at a constant SEI of 96 kJ/L. Ozkan et al reported that increasing discharge frequency from 16.2 to 28.6 kHz slightly decreased both CO_2 conversion (22.0% to 17.5%) and energy efficiency (15.3% to 12.5 %) at a discharge power of 55 W and a CO_2 flow rate of 200 mL/min in a DBD reactor [37]. They found that the decrease in CO_2 conversion by rising the frequency of discharge was not induced by the produced microdischarge, as the change of the discharge frequency did not change the number and lifetime of the microdischarge in the reaction. They believed that the drop in CO_2 conversion was mainly resulted from the decrease in the gas voltage by increasing the discharge frequency [37]. Liu et al demonstrated that the discharge frequency was the least important operating parameter affecting the plasma conversion of CH_4 in a DBD reactor [21]. They found that the conversion of CH_4 slightly decreased (by 10%) when rising the frequency from 20 to 50 kHz at a fixed discharge power of 45 W and a CO_2 flow rate of 100 mL/min [21].

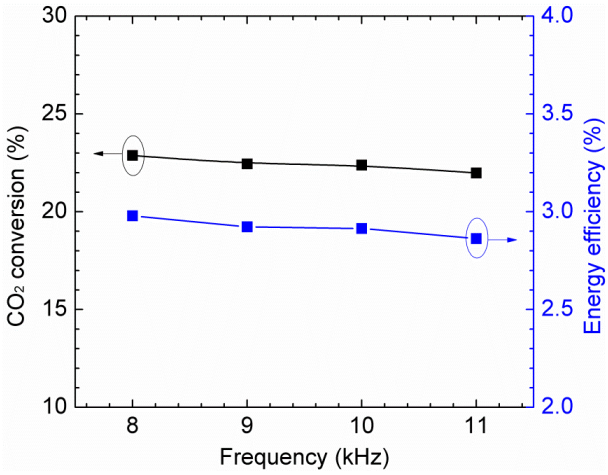

Fig. 2. Effect of discharge frequency on CO_2 conversion and energy efficiency (SEI: 96 kJ/L; feed flow rate: 25 mL/min; discharge length: 100 mm; discharge gap: 2.5 mm).

Fig. 3 shows the effect of discharge frequency on the selectivity of CO and carbon balance. Increasing the discharge frequency from 8 to 11 kHz showed a negligible effect on the CO selectivity. The selectivity of CO reached nearly 100%, which indicated that CO was the major product from CO_2 decomposition and the stoichiometric conversion of CO_2 into CO was achieved. Moreover, the carbon balance was also independent of the frequency and changed between 98.7% and 99.2%. Carbon deposition was not observed and detected during the plasma CO_2 reaction. It is noticeable that the CO selectivity and carbon balance were also independent of the other processing parameters (e.g. CO_2 flow rate, discharge power, discharge gap, discharge length and thickness of dielectric material). Therefore, the influence of plasma processing parameters on the plasma conversion of CO_2 will be only discussed in terms of the conversion of CO_2 and energy efficiency in the following sections.

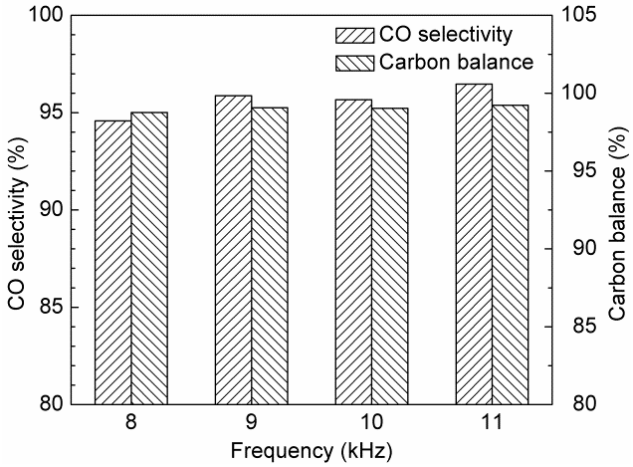

Fig. 3. Effect of discharge frequency on CO selectivity (SEI: 96 kJ/L; feed flow rate: 25 mL/min; discharge length: 100 mm; discharge gap: 2.5 mm).

3.2 Effect of discharge power and feed flow rate

Fig. 4 shows the influence of discharge power on the conversion of CO_2 and energy efficiency. Increasing discharge power increased the conversion of CO_2, but decreased the energy efficiency. CO_2 conversion increased from 17.4% to 22.4% as the plasma power changed from 10 to 50 W. The discharge power was controlled by changing the applied voltage at a constant frequency. The increase of the plasma power increased both the magnitude and number of the current pulses, as shown in Fig. 5. This

phenomenon indicated that the number of microdischarges was increased by increasing the discharge power, suggesting the production of more chemical reaction channels and reactive species for CO_2 processing, resulted in the enhanced CO_2 conversion. This finding was observed in previous works related to plasma chemical reactions [35, 61, 62]. Although higher power led to the enhanced CO_2 conversion, the efficiency of the reaction was decreased from 9.0% to 2.3% when changing the plasma power from 10 to 50 W.

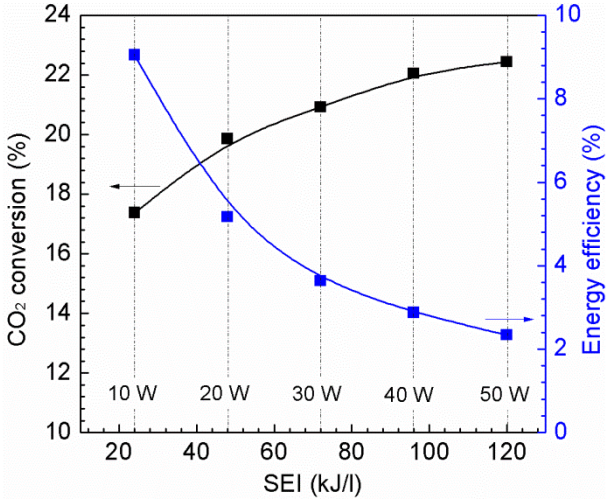

Fig. 4. Effect of discharge power and SEI on CO_2 conversion and energy efficiency (CO_2 flow rate: 25 mL/min; discharge length: 100 mm; discharge gap: 2.5 mm).

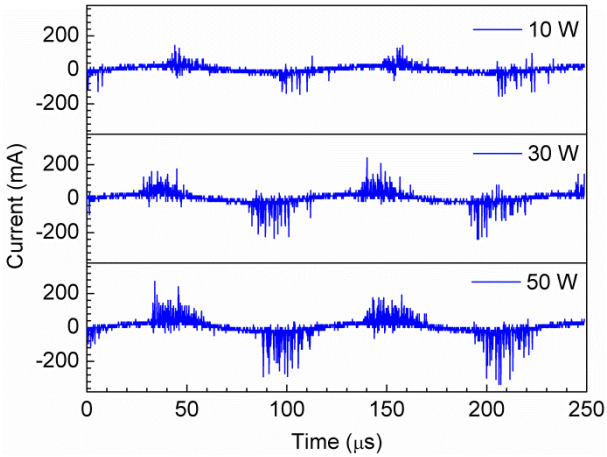

Fig. 5. Effect of discharge power on the current signals (feed flow rate: 25 mL/min; discharge length: 100 mm; discharge gap: 2.5 mm).

The effect of CO_2 flow rate on CO_2 conversion and process efficiency is shown in Fig. 6. Clearly, a maximum CO_2 conversion of 22.4% was obtained at the minimum CO_2 flow rate of 25 mL/min. With the other processing parameters fixed, increasing CO_2 flow rate reduced the residence time of the reactants in the plasma, which decreased the possibility for CO_2 decomposition through the collisions with electrons and chemically reactive species, and consequently lowered the conversion of CO_2. For example, the residence time of CO_2 in the DBD decreased from 36.8 to 7.4 s when the CO_2 flow varied from 25 to 125 mL/min, which decreased the conversion of CO_2 from its maximum value to 12.6%. Although increasing the feed flow rate decreased the CO_2 conversion, the concentration of converted CO_2 increased. Therefore, the energy efficiency of the reaction was increased from 2.3% to 6.6% by increasing the feed flow rate from 25 to 125 mL/min.

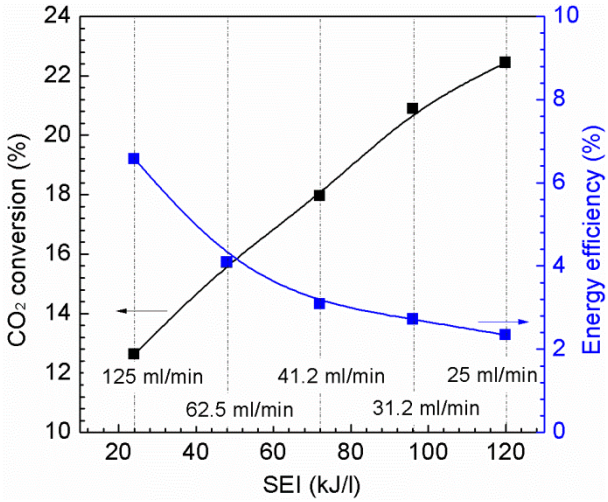

Fig. 6. Effect of feed flow rate and SEI on CO_2 conversion and energy efficiency (discharge power: 50W; discharge length: 100 mm; discharge gap: 2.5 mm).

From the definition of SEI (Eq. (5)), the variation of SEI can be achieved by changing the discharge power and/or feed flow rate. In Fig. 4 and Fig. 6, the increase of SEI from 24 to 120 kJ/L was obtained by two approaches: (1) increasing the plasma power from 10 to 50 W at a constant CO_2 flow rate of 25 mL/min; (2) decreasing the CO_2 flow from 125 to 25 mL/min by fixing the discharge power at 50 W. Clearly, how do we change the SEI has a different influence on the CO_2 conversion and reaction efficiency. For example, the CO_2 conversion was increased by 28.7% (from 17.4% to 22.4%) when

increasing the SEI from 24 to 120 kJ/L by changing the discharge power (Fig. 4), whilst the conversion of CO_2 was enhanced by 77.8% (from 12.6% to 22.4%) when changing the SEI using the second approach (Fig. 6). Clearly, the residence time of CO_2 in the discharge was quite different using these two approaches. These results clearly showed that changing the SEI by changing the CO_2 flow has a more pronounced influence on CO_2 conversion compared to the change of discharge power. By contrast, the plasma power plays a more important role in determining the efficiency of the plasma CO_2 conversion. Therefore, both plasma power and CO_2 flow rate should be considered when pursuing a suitable SEI for high CO_2 conversion and energy efficiency simultaneously.

3.3 Effect of discharge gap and discharge length

Fig. 7 shows the effect of changing discharge gap on the conversion of CO_2. At a constant SEI, increasing the discharge gap reduced both energy efficiency and CO_2 conversion. For example, the conversion of CO_2 decreased from 22.1% to 16.8% when the discharge gap increased from 2.5 to 3.5 mm. Similarly, the energy efficiency for plasma CO_2 conversion was decreased by 25% when changing the discharge gap from 2.5 to 3.5 mm. Increasing discharge gap could increase the residence time of the reactants in the plasma, which can have a positive effect on the CO_2 conversion. However, increasing the discharge gap decreases the power density (defined as discharge power/discharge volume) at a constant discharge power due to the increased plasma volume. At a larger gap, it is more likely to form a "partial discharging" rather than a "fully-bridged" discharge as the streamers cannot fully cover the discharge volume, resulted in a reduced CO_2 conversion. In this study, this negative effect is more prominent in the conversion of CO_2 compared to the positive effect due to the increased residence time. In addition, increasing the gap from 2.5 to 3.5 mm slightly decreased the transferred charge, and consequently reduced the production of electrons and reactive species, as shown in Fig. 8 [63].

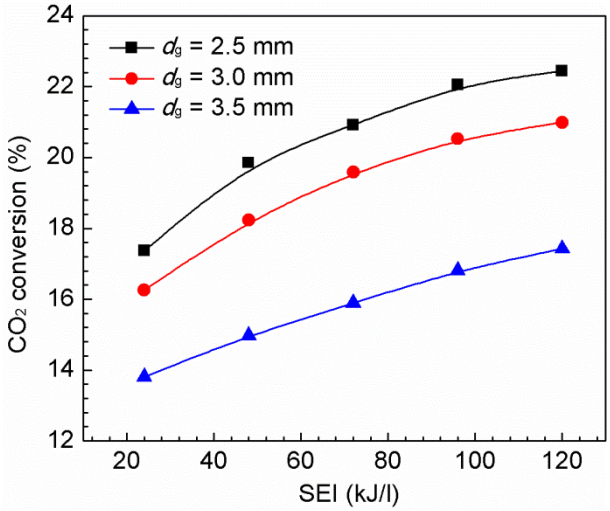

(a)

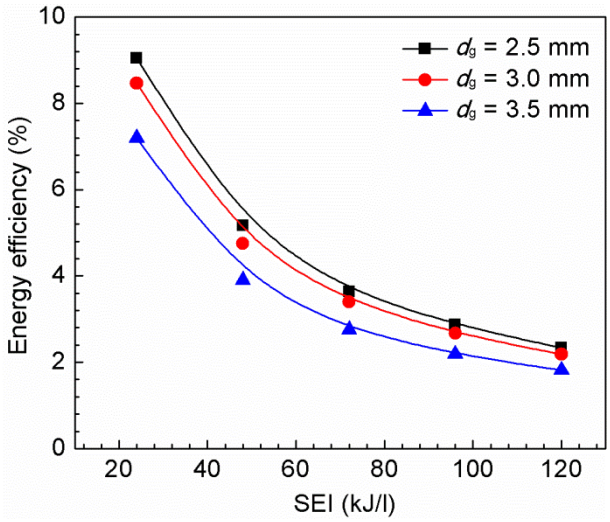

(b)

Fig. 7. Effect of discharge gap on CO_2 conversion and energy efficiency (feed flow rate: 25 mL/min; discharge length: 100 mm).

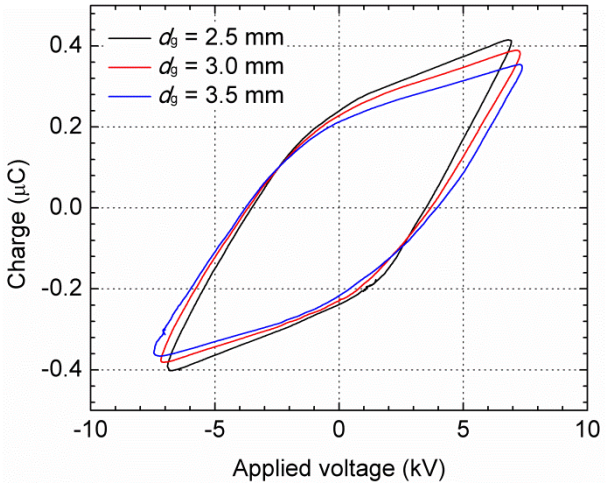

Fig. 8. Lissajous figures of the CO_2 DBD with different discharge gaps at a constant SEI of 96 kJ/L (discharge length: 100 mm, CO_2 feed flow rate: 25 mL/min; frequency: 9 kHz).

The influence of SEI and discharge length on plasma processing of CO_2 is displayed in Fig. 9. Both CO_2 conversion and energy efficiency increased by around 27% as the discharge length increased from 60 to 140 mm at a SEI of 120 kJ/L. The influence of discharge length on the CO_2 conversion can be attributed to two competing effects. Firstly, increasing the discharge length from 60 to 140 mm significantly increased the residence time of CO_2 in the plasma by 133.3%, which positively affect the conversion of CO_2 (e.g. enhancing CO_2 conversion) due to the increased probability of CO_2 molecules colliding with highly energetic electrons and reactive species. However, increasing the discharge length from 60 to 140 mm increased the surface area of the dielectric material (i.e. quartz tube) from 47.1 to 110.0 cm^2, leading to the increased energy loss due to the heat dissipation [64]. Moreover, increasing discharge length also reduced the plasma power density owing to the enlarged plasma volume (from 9.2 to 21.4 cm^3) at a fixed discharge power [64]. These effects tend to negatively affect the conversion of CO_2. In this study, increasing the discharge length significantly increased the residence time of CO_2 in the reaction, which plays a more dominant role in the conversion of CO_2 compared to the negative effects (e.g. reduced power density and increased energy loss) caused by the increased discharge length, thus increasing the CO_2 conversion as shown in Fig.9.

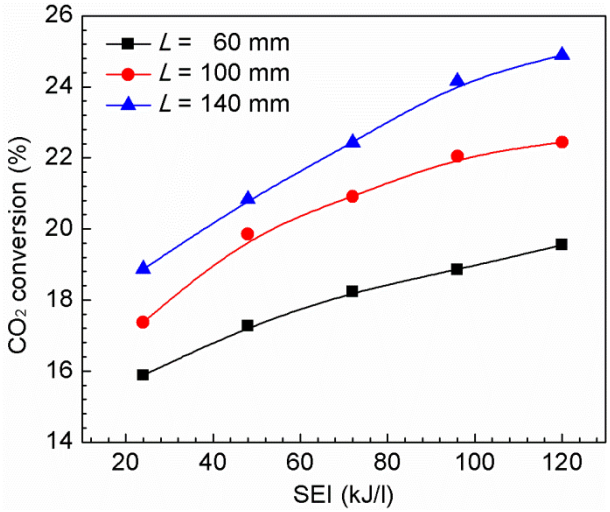

(a)

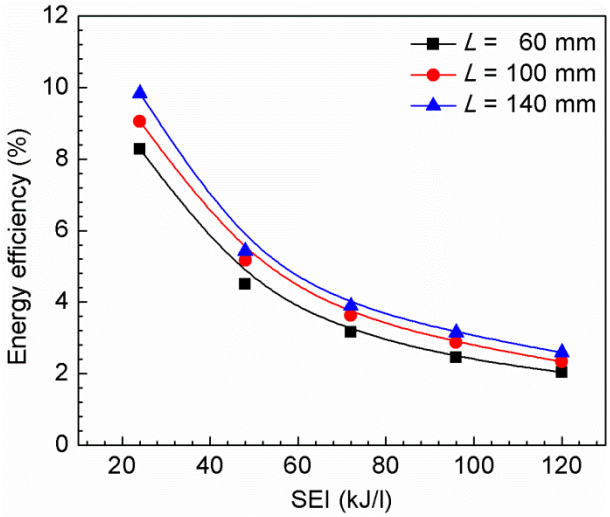

(b)

Fig. 9. Effect of discharge length on CO_2 conversion and energy efficiency (feed flow rate: 25 mL/min; discharge gap: 2.5 mm).

3.4 Effect of thickness of dielectric material

Fig. 10 shows the influence of thickness of dielectric material on the plasma CO_2 conversion as a function of SEI. Clearly, increasing the thickness of the quartz tube decreased the conversion of CO_2 and reaction efficiency at a fixed SEI. For example, both the CO_2 conversion and energy efficiency were decreased by ~15.0% when changing the thickness of dielectric material from 1.5 to 2.5 mm at a SEI of 120 kJ/L. In this study, the plasma gap was maintained at 2.5 mm by simultaneously changing the dimension of the quartz tube and inner electrode with a constant external diameter of the quartz tube. In this way, the discharge volume was decreased by 10.3% when increasing the thickness of dielectric material from 1.5 to 2.5 mm, resulted in the decreased residence time of CO_2 in the DBD. Furthermore, we find that increasing the thickness of quartz tube (from 1.5 to 2.5 mm) decreased the transferred charge by 19.9%, which decreased the generation of electrons for CO_2 conversion [63]. Therefore, the decreased residence time and transferred charge by increasing the thickness of dielectric material is of greater importance to determine the conversion of CO_2 in our DBD reactor.

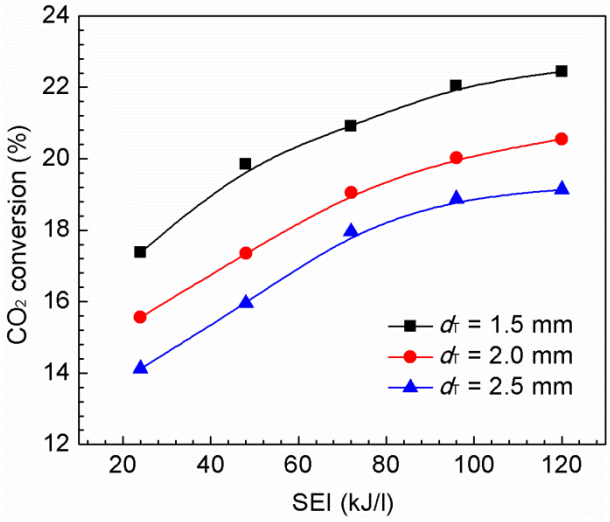

(a)

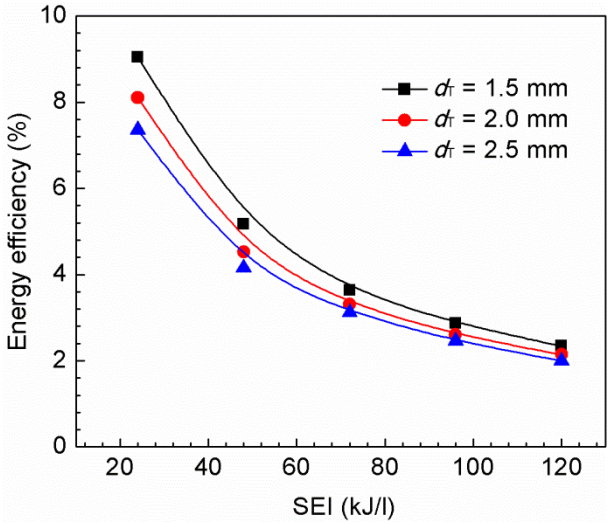

(b)

Fig. 10. Effect of the thickness of dielectric material on CO_2 conversion and energy efficiency (feed flow rate: 25 mL/min; discharge gap: 2.5 mm; discharge length: 100 mm).

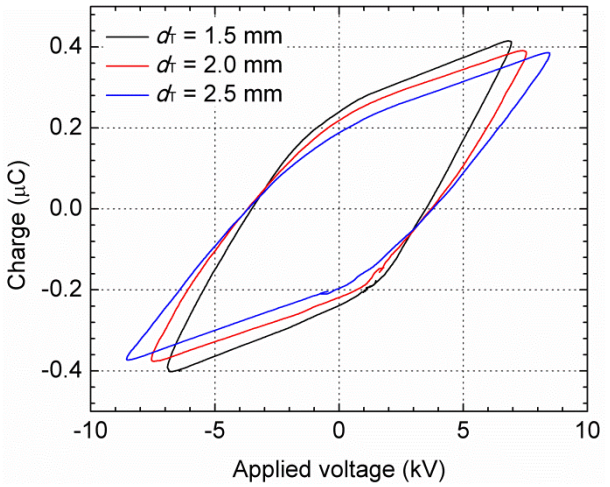

Fig. 11. Lissajous figures of the CO_2 DBD with different thicknesses of dielectric material at a constant SEI of 96 kJ/L (discharge gap: 2.5 mm, discharge length: 100 mm; frequency: 9 kHz).

3.5 Regression models for the plasma process performance estimation

The performance of CO_2 conversion in a DBD plasma system is closely associated with a variety of plasma and operating parameters. In this work, the regression models were developed to determine how these different plasma and operating parameters affect the plasma processing of CO_2. In these models, the dependent variables were CO_2 conversion (C_{CO_2}) and energy efficiency (η), while the independent variables were discharge frequency (f), discharge power (P), feed flow rate (q), discharge length (L), discharge gap (d_g) and thickness of dielectric material (d_T), as shown in Eq. (7) and Eq. (8).

$$C_{CO_2} = K_1 [f]^{a_1} [P]^{b_1} [q]^{c_1} [L]^{d_1} [d_g]^{e_1} [d_T]^{f_1} \quad (7)$$

$$\eta = K_2 [f]^{a_2} [P]^{b_2} [q]^{c_2} [L]^{d_2} [d_g]^{e_2} [d_T]^{f_2} \quad (8)$$

where K_1 and K_2 are the constants that correlate the reaction performance (CO_2 conversion and energy efficiency) with the processing parameters. a_i, b_i, c_i, d_i, e_i, and f_i (i=1 and 2) are the exponent of the term related to each processing parameter. The value of these constants and indexes were calculated by the regression analysis method using IBM SPSS statistics version 24. The empirical models are expressed in Eq. (9) and Eq. (10). These two models were determined based on the experimental results under the following operating conditions: f = 8-11 kHz, P = 10-50 W, q = 25-125 mL/min, L = 60-140 mm, d_g = 2.5-3.5 mm and d_T = 1.5-2.5 mm. The experimental results agreed with the predicted data with a maximum relative error of ~5.7% for the conversion of CO_2 and process efficiency. This high accuracy can be confirmed by the high value of R^2 (0.9872 for CO_2 conversion; 0.9947 for energy efficiency).

$$C_{CO_2} = 34.3401 \times [f]^{-0.0448} [P]^{0.1634} [q]^{-0.3839} [L]^{0.2527} [d_g]^{-0.6999} [d_T]^{-0.3593}, \ R^2=0.9872 \quad (9)$$

$$\eta = 6.4876 \times [f]^{-0.0415} [P]^{-0.8367} [q]^{0.6158} [L]^{0.2531} [d_g]^{-0.7004} [d_T]^{-0.3605}, \ R^2=0.9947 \quad (10)$$

The standardized coefficient can be used to understand the relative significance of a parameter on the plasma CO_2 conversion. It indicates the average standard change in the conversion of CO_2 and process efficiency of conversion reaction associated with a standard change in one processing parameter while

keeping other parameters constant [65]. The positive standardized coefficient suggests that the conversion of CO_2 and efficiency of the reaction increase by increasing the corresponding processing parameter.

Fig. 12 shows the standardized coefficient of each processing parameter in the regression models for the conversion of CO_2. Clearly, the plasma power and discharge length positively affected the conversion of CO_2; while the discharge frequency, feed flow rate, discharge gap and dielectric material thickness had a negative influence on CO_2 conversion. The absolute value of the standardized coefficient for the feed flow rate was comparable to that for the discharge power, and followed by these for the discharge gap, discharge length, thickness of dielectric material and discharge frequency. Therefore, the relative significance of the processing parameters on CO_2 conversion follows the order of $q \approx P > d_g > L > d_T > f$.

As shown in Fig. 12, the energy efficiency for the conversion of CO_2 was positively correlated to CO_2 flow rate and discharge length, but was negatively affected by the discharge power, discharge gap and dielectric material thickness. The influence of the discharge frequency on the efficiency of plasma CO_2 conversion was negligible. Due to the highest absolute value of the standardized coefficient, the plasma power showed a more significant effect on the energy efficiency for CO_2 splitting compared with other processing parameters. Briefly, the relative significance of these processing parameters on energy efficiency is $P > q > d_g > d_T > L > f$.

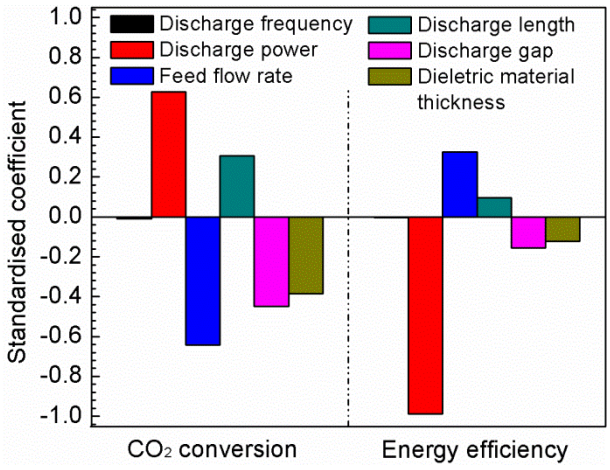

Fig. 12. Standardized coefficients of different processing parameters for CO_2 conversion (left) and energy efficiency (right)

3.6 Effect of reactor design on CO_2 conversion

Fig. 13 shows the influence of different inner and outer electrodes on the conversion of CO_2. The CO_2 decomposition and process efficiency were enhanced by around 10.8% at a SEI of 120 kJ/L when the SS mesh outer electrode was replaced by Al foil. Compared to SS mesh, the use of Al foil as the outer electrode covered the outer surface of the quartz tube more uniformly and increases the effective discharge area. As a result, the number of micro-discharges generated in the discharge increased, which contributes to the enhanced CO_2 decomposition and process efficiency.

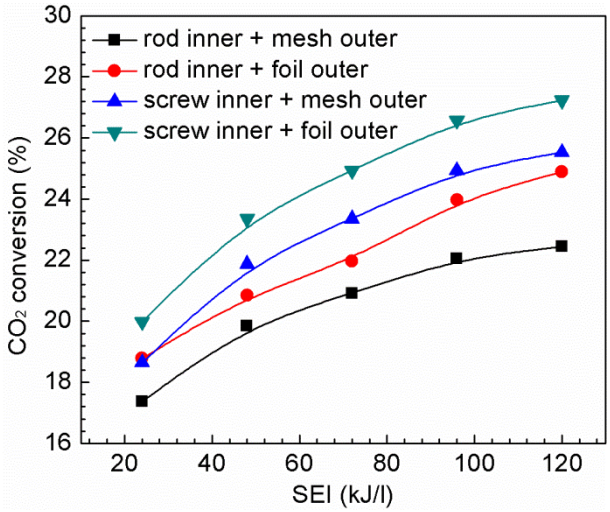

(a)

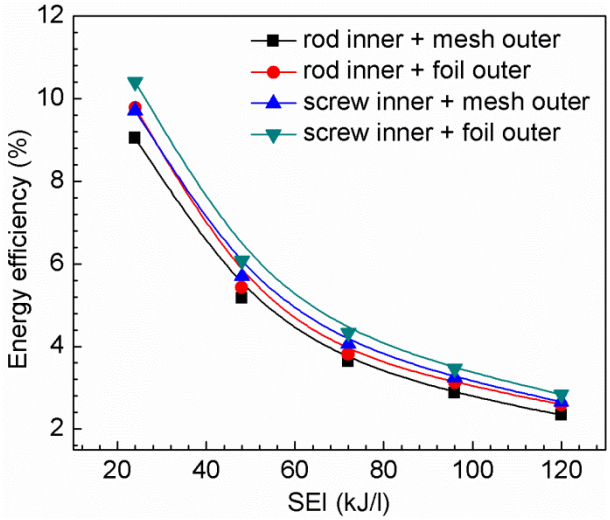

(b)

Fig. 13. Effect of inner and outer electrode forms on CO_2 conversion and energy efficiency (feed flow rate: 25 mL/min; discharge gap: 2.5 mm; discharge length: 100 mm).

Clearly, increasing the SEI from 24 to 120 kJ/L increased the conversion of CO_2 regardless of the electrodes used. Compared to the SS rod electrode, the use of the SS screw-type inner electrode enhanced the CO_2 conversion and energy efficiency by 12-14% at a fixed SEI of 120 kJ/L (Fig. 14). The sharp edge of the SS screw-type electrode could distort the electric field in the discharge and enhance the local electric field near the inner electrode, and consequently generates more intensified filaments near the shape edge of the screw electrode (Fig. 14). This effect could generate more reaction channels which makes a significant contribution to the enhanced reaction performance (e.g. CO_2 conversion).

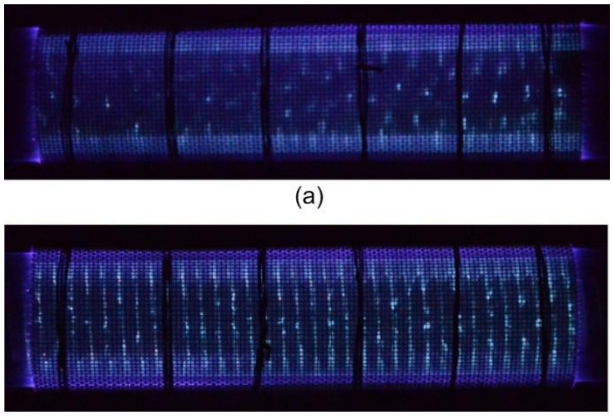

Fig. 14. Images of the CO_2 DBD plasma (exposure time: 25 ms): (a) SS rod inner electrode; (b) SS screw-type inner electrode (discharge power: 40 W; discharge gap: 2.5 mm, discharge length: 100 mm; CO_2 feed flow rate: 25 mL/min; frequency: 9 kHz; outer electrode: SS mesh).

The combination of the SS screw-type inner electrode and Al foil outer electrode showed the highest CO_2 conversion and energy efficiency in our DBD reactor: 27.2% for CO_2 conversion and 2.8% for energy efficiency at a SEI of 120 kJ/L. The maximum energy efficiency of 10.4% was achieved at a low SEI of 24 kJ/L using these two electrodes. Fig. 15 shows the voltage and current signals of CO_2 discharges with different electrodes at a SEI of 96 kJ/L. Clearly, the currents were quasi-sinusoid with a large number of current peaks in each half cycle. These current peaks were reflected by the formation of transient filamentary microdischarges in the CO_2 DBD. When the SS mesh outer electrode was replaced by the Al foil, the filaments extended across the electrode gap due to larger effective discharge area, evidenced by increased number and amplitude of the current pluses (Fig. 15 (b)). When the SS screw-type

inner electrode was used, the current pulses were also intensified due to the formation of higher local electric field resulting from the sharp edge of the screw-type electrode (Fig. 15 (c)). The amplitude and number of the current pulses and microdischarges, as well as the transferred charge were further enhanced by the combination of the Al foil outer electrode and SS screw-type inner electrode in the DBD reactor (Fig. 15 (d) and Fig. 16), creating more reaction channels to further enhanced the reaction performance of the plasma CO_2 conversion.

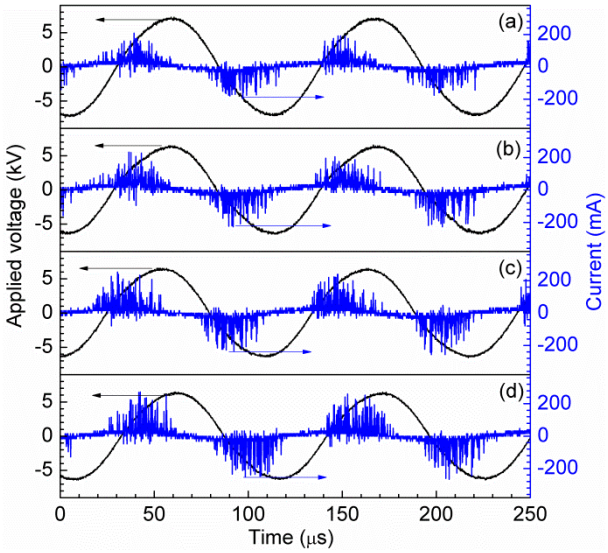

Fig. 15. Electrical signals of the CO_2 DBD: (a) SS mesh outer electrode and SS rod inner electrode; (b) Al foil outer electrode and SS rod inner electrode; (c) SS mesh outer electrode and SS screw-type inner electrode; (d) Al foil outer electrode and SS screw-type inner electrode (SEI: 96 kJ/L; discharge gap: 2.5 mm, discharge length: 100 mm; CO_2 feed flow rate: 25 mL/min; frequency: 9 kHz).

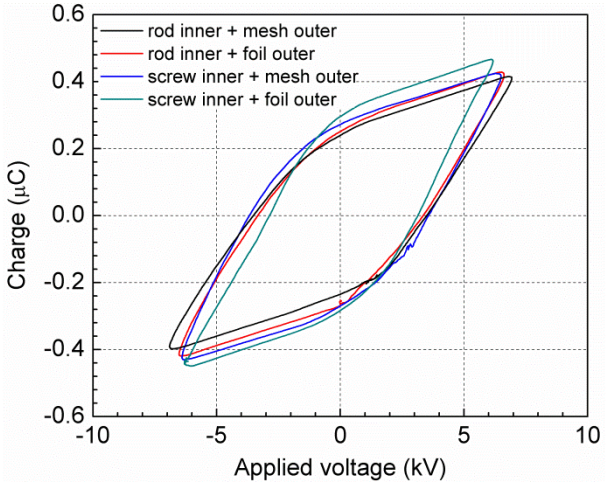

Fig. 16. Lissajous figures of the CO_2 DBD with different electrodes (SEI: 96 kJ/L; discharge gap: 2.5 mm;

discharge length: 100 mm; frequency: 9 kHz).

3.7 Discussion

Table 2 compares the maximum conversion of CO_2 and energy efficiency of the plasma process using different atmospheric plasma sources. The conversion of highly diluted CO_2 in the atmospheric pressure plasmas was not included in Table 2 due to the use of expensive dilution gas, especially He. In the plasma process, a trade-off effect exists between the conversion of CO_2 and reaction efficiency [35]. In general, higher SEI generates higher CO_2 conversion but lowers the energy efficiency of plasma process, while higher energy efficiency with lower CO_2 conversion can be obtained at a lower SEI. To solve this problem, further modification of the plasma system and optimisation of the plasma process is required. One such modification could be the improvement of plasma system design, as this work shows the combination of the Al foil outer electrode and SS screw-type inner electrode can improve both CO_2 conversion and energy efficiency. In this work, the highest energy efficiency of 10.4% was achieved in the conversion of CO_2 with a CO_2 conversion of 20% at a plasma power of 10 W and a CO_2 flow of 50 mL/min. The other improvement of the reaction performance might be achieved through the addition of a suitable catalyst into the plasma, as a hybrid plasma-catalytic process has significant potential to form a low temperature synergistic effect, resulted in higher CO_2 conversion whilst maintaining low energy consumption, creating a more attractive process for the utilization of CO_2 on an industrial scale. However, very limited work has been devoted to investigate the plasma-catalytic decomposition of CO_2 into CO and oxygen as very limited knowledge of such catalysts can be found from conventional catalytic processes. Our recent work successfully demonstrated the combination of DBD with $BaTiO_3$ and TiO_2 photocatalysts significantly enhanced the decomposition of CO_2 and process efficiency for CO_2 conversion at low temperatures [45]. All the photocatalysts were placed along the bottom of the DBD reactor in the plasma discharge area, resulted in effective plasma-catalyst interactions. The results showed that electron induced photocatalytic reaction might play an important role in the enhancement of the process performance besides the positive physical effect due to the interactions between the catalysts and plasma such as the enhancement of the local electrical field and average electric field. Chen et al reported

that CO_2 conversion and energy efficiency could be doubled when using a plasma pretreated NiO/TiO_2 catalyst in a pulsed-wave sustained microwave discharge [53]. Modification of metal electrodes with the coating of Cu, Rh, Pt, Au and Pd were investigated in the conversion of CO_2 diluted with He, Ar or N_2 in a glow discharge [55, 66, 67]. The maximum CO_2 conversion of 36.4% was obtained with the Rh coated electrode [55]. Non-catalytic packing materials (e.g. Al_2O_3) have shown the enhanced reaction performance in plasma-assisted environmental clean-up such as the removal or oxidation of gas pollutants. However, these materials have a very limited effect on the plasma synthesis of fuels and chemicals such as methane conversion or CO_2 conversion. Previous works also showed changing the dielectric material in a DBD reactor might open a new route to tailor the formation of a range of active species and change the chemical reactions. Li et al evaluated the effect of $Ca_{0.7}Sr_{0.3}TiO_3$ (as a dielectric material) on CO_2 conversion in a DBD reactor [38, 68, 69]. Intensified microdischarges with stronger current pulses were generated due to high permittivity of $Ca_{0.7}Sr_{0.3}TiO_3$ ceramic, leading to a higher CO_2 conversion compared to that of the plasma process using alumina and silica glass. Wang et al carried out similar research using $Ca_{0.8}Sr_{0.2}TiO_3$ added with $CaO\text{-}B_2O_3\text{-}SiO_2$ (CBS) glass as a dielectric material. The maximum CO_2 conversion of 48.7% was achieved with an addition of 5% CBS [39].

Table 2. Comparison of CO_2 conversion and energy efficiency using different atmospheric pressure plasma sources.

Plasma type	Packing materials/ Catalysts	Maximum CO_2 conversion			Maximum energy efficiency			Ref
		SEI (kJ/L)	CO_2 conversion (%)	Energy efficiency (%)	SEI (kJ/L)	CO_2 conversion (%)	Energy efficiency (%)	
DBD	-	120	27.2	2.8	24	20.0	10.4	This work
DBD	-	229.0	34.0	1.9	4.3	3.1	8.0	[30]
DBD	-	297.6	46.6	2.0	1.6	2.3	17.7	[33]
DBD	-	60.0	18.2	1.7	20.0	9.6	3.8	[31]
GAD	-	15.4	17.4	14.1	9.8	15.2	19.3	[47]
DBD	-	22.2	24.3	12.6	11.7	16.0	15.7	[36]
DBD	-	240.0	30.0	1.6	45.1	14.0	3.9	[27]
Corona	-	80	10.9	1.7	5.2	3.1	7.5	[50]
Microwave	NiO/TiO_2 (Ar plasma	-	-	-	30	41.3	17.2	[53]

	treated)							
DBD	$BaTiO_3$	-	-	-	28	38.3	16.6	[45]
Packed bed DBD	CaO	75.8	41.9	5.7	45.5	32.9	7.1	[42]
Packed bed DBD	ZrO_2	240	42.3	4.6	36	9.6	9.6	[43]
Packed bed DBD	$CaTiO_3$	52.9	20.5	4.8	32.4	15.8	6.1	[40]
Packed bed DBD	$BaTiO_3$	60.0	28.2	5.9	24.0	13.7	7.1	[13]

4. Conclusions

The effects of different plasma and processing parameters (plasma power, discharge length, discharge frequency, CO_2 flow rate, electrode gap, and thickness of dielectric material) and reactor design on the conversion of CO_2 were investigated in a coaxial DBD reactor. The discharge frequency showed a weak effect on CO_2 decomposition and process efficiency. Higher CO_2 conversion can be obtained by increasing the discharge power and/or decreasing the feed flow rate; while the decrease in discharge power and/or increase in feed flow rate led to a higher energy efficiency. Clearly, a trade-off effect exists between the conversion of CO_2 and efficiency of the plasma process. In addition, decreasing the discharge gap and thickness of dielectric material and/or enlarging discharge length positively affected both CO_2 decomposition and energy efficiency. From the regression models, we can find that the feed flow rate and discharge power are the key for CO_2 conversion; while the discharge power significantly affects the process efficiency for CO_2 conversion. In addition, the use of the Al foil outer electrode and SS screw-type inner electrode significantly enhanced the conversion of CO_2 and energy efficiency compared to other electrode forms. The highest CO_2 conversion (27.2%) was achieved at a SEI of 120 kJ/L, while the maximum process energy efficiency (10.4%) was obtained at a SEI of 24 kJ/L. The use of the SS screw-type inner electrode could initiate enhanced local electric field near sharp edge of the electrode, while the use of Al foil as an outer electrode could enlarge the effectiveness of discharge area compared to a mesh electrode. Both effects contributed to the enhanced process performance for CO_2 conversion and utilization.

Acknowledgement

The financial support of this work by the EPSRC SUPERGEN Hydrogen & Fuel Cell (H2FC) Programme (EP/J016454/1, Ref EACPR_PS5768) is gratefully acknowledged.

Reference

[1] The State of Greenhouse Gases in the Atmosphere Based on Global Observations through 2013. WMO Greenhouse Gas Bulletin: World Meteorological Organization; 2014. p. 1-10.
[2] Climate Change 2014, Synthesis Report, Summary for Policymakers
[3] Climate Change Act 2008 http://www.legislation.gov.uk/ukpga/2008/27/contents.
[4] J. Gibbins, H. Chalmers, Energ. Policy. 36 (2008) 4317-4322.
[5] S. Bachu, Prog. Energ. Combust. 34 (2008) 254-273.
[6] E.V. Kondratenko, G. Mul, J. Baltrusaitis, G.O. Larrazabal, J. Perez-Ramirez, Energ. Environ. Sci. 6 (2013) 3112-3135.
[7] M. Mikkelsen, M. Jorgensen, F.C. Krebs, Energ. Environ. Sci. 3 (2010) 43-81.
[8] R.W. Dorner, D.R. Hardy, F.W. Williams, H.D. Willauer, Energ. Environ. Sci. 3 (2010) 884-890.
[9] J. Qiao, Y. Liu, F. Hong, J. Zhang, Chem. Soc. Rev. 43 (2014) 631-675.
[10] K.F. Li, X.Q. An, K.H. Park, M. Khraisheh, J.W. Tang, Catal. Today 224 (2014) 3-12.
[11] P. Lahijani, Z.A. Zainal, M. Mohammadi, A.R. Mohamed, Renew. Sust. Energ. Rev. 41 (2015) 615-632.
[12] J. Medina-Ramos, R.C. Pupillo, T.P. Keane, J.L. DiMeglio, J. Rosenthal, J. Am. Chem. Soc. 137 (2015) 5021-5027.
[13] D. Mei, X. Zhu, Y.L. He, J.D. Yan, X. Tu, Plasma Sources Sci. Technol. 24 (2015) 015011.
[14] X. Tu, J.C. Whitehead, Appl. Catal. B-Environ. 125 (2012) 439-448.
[15] A. Wu, X. Li, L. Chen, F. Zhu, H. Zhang, C. Du, et al. Int. J. Hydrogen Energ. 40 (2015) 9039-9048.
[16] F. Zhu, X. Li, H. Zhang, A. Wu, J. Yan, M. Ni, et al. Fuel. 176 (2016) 78-85.
[17] H.J. Gallon, X. Tu, M.V. Twigg, J.C. Whitehead, Appl. Catal. B-Environ. 106 (2011) 616-620.
[18] X. Tu, J.C. Whitehead, Int. J. Hydrogen Energ. 39 (2014) 9658-9669.
[19] H. Zhang, C. Du, A. Wu, Z. Bo, J. Yan, X. Li, Int. J. Hydrogen Energ. 39 (2014) 12620-12635.
[20] H. Zhang, F. Zhu, X. Li, K. Cen, C. Du, X. Tu, RSC Adv. 6 (2016) 12770-12781.
[21] S.Y. Liu, D.H. Mei, Z. Shen, X. Tu, J. Phys. Chem. C 118 (2014) 10686-10693.
[22] S. Liu, D. Mei, L. Wang, X. Tu, Chem. Eng. J. 307 (2017) 793-802.
[23] L. Wang, S.Y. Liu, C. Xu, X. Tu, Green Chem. 18 (2016) 5658-5666.
[24] Y. Zeng, X. Zhu, D. Mei, B. Ashford, X. Tu, Catal. Today 256 (2015) 80-87.

[25] D. Mei, B. Ashford, Y.-L. He, X. Tu, Plasma Process. Polym. (2016) DOI: 10.1002/ppap.201600076.
[26] R. Snoeckx, Y.X. Zeng, X. Tu, A. Bogaerts, RSC Adv. 5 (2015) 29799-29808.
[27] S. Paulussen, B. Verheyde, X. Tu, C. De Bie, T. Martens, D. Petrovic, et al. Plasma Sources Sci. Technol. 19 (2010) 034015.
[28] R. Aerts, R. Snoeckx, A. Bogaerts, Plasma Process. Polym. 11 (2014) 985-992.
[29] F. Brehmer, S. Welzel, M.C.M. van de Sanden, R. Engeln, J. Appl. Phys. 116 (2014) 123303.
[30] R. Aerts, W. Somers, A. Bogaerts, ChemSusChem. 8 (2015) 702-716.
[31] X. Duan, Y. Li, W. Ge, B. Wang, Greenh. Gases. 5 (2015) 131-140.
[32] M. Ramakers, I. Michielsen, R. Aerts, V. Meynen, A. Bogaerts, Plasma Process. Polym. 12 (2015) 755-763.
[33] I. Belov, S. Paulussen, A. Bogaerts, Plasma Sources Sci. Technol. 25 (2016) 015023.
[34] I. Belov, J. Vanneste, M. Aghaee, S. Paulussen, A. Bogaerts, Plasma Process. Polym. (2016) DOI: 10.1002/ppap.201600065.
[35] D.H. Mei, Y.-L. He, S.Y. Liu, J.D. Yan, X. Tu, Plasma Process. Polym. 13 (2016) 544-556.
[36] A. Ozkan, T. Dufour, A. Bogaerts, F. Reniers, Plasma Sources Sci. Technol. 25 (2016) 045016.
[37] A. Ozkan, T. Dufour, T. Silva, N. Britun, R. Snyders, A. Bogaerts, et al. Plasma Sources Sci. Technol. 25 (2016) 025013.
[38] R.X. Li, Q. Tang, S. Yin, T. Sato, Appl. Phys. Lett. 90 (2007) 131502.
[39] S. Wang, Y. Zhang, X. Liu, X. Wang, Plasma Chem. Plasma Process. 32 (2012) 979-989.
[40] Q.Q. Yu, M. Kong, T. Liu, J.H. Fei, X.M. Zheng, Plasma Chem. Plasma Process. 32 (2012) 153-163.
[41] M.A. Lindon, E.E. Scime, Front. Phys. 2 (2014) Article 55.
[42] X.F. Duan, Z.Y. Hu, Y.P. Li, B.W. Wang, AIChE J. 61 (2015) 898-903.
[43] K. Van Laer, A. Bogaerts, Energy Technol. 3 (2015) 1038-1044.
[44] T. Butterworth, R. Elder, R. Allen, Chem. Eng. J. 293 (2016) 55-67.
[45] D. Mei, X. Zhu, C. Wu, B. Ashford, P.T. Williams, X. Tu, Appl. Catal. B-Environ. 182 (2016) 525-532.
[46] D. Ray, C. Subrahmanyam, RSC Adv. 6 (2016) 39492-39499.
[47] A. Indarto, D.R. Yang, J.W. Choi, H. Lee, H.K. Song, J. Hazard. Mater. 146 (2007) 309-315.
[48] S.C. Kim, M.S. Lim, Y.N. Chun, Plasma Chem. Plasma Process. 34 (2014) 125-143.
[49] T.G. Nunnally, K. Gutsol, A. Rabinovich, A. Fridman, A. Gutsol, A. Kemoun, J. Phys. D-Appl. Phys. 44 (2011) 274009.
[50] W. Xu, M.W. Li, G.H. Xu, Y.L. Tian, Jpn. J. Appl. Phys. 43 (2004) 8310-8311.
[51] G. Horvath, J.D. Skalny, N.J. Mason, J. Phys. D-Appl. Phys. 41 (2008) 225207.
[52] H.S. Uhm, H.S. Kwak, Y.C. Hong, Environ. Pollut. 211 (2016) 191-197.

[53] G.X. Chen, V. Georgieva, T. Godfroid, R. Snyders, M.-P Delplancke-Ogletree, Appl. Catal. B-Environ. 190 (2016) 115-124.
[54] P.G. Reyes, E.F. Mendez, D. Osorio-Gonzalez, F. Castillo, H. Martinez, Phys, Status, Solidi, C. 5 (2008) 907-910.
[55] S.L. Brock, T. Shimojo, M. Marquez, C. Marun, S.L. Suib, H. Matsumoto, et al. J. Catal. 184 (1999) 123-133.
[56] U. Kogelschatz, Plasma Chem. Plasma Process. 23 (2003) 1-46.
[57] N. Jiang, J. Hu, J. Li, K.F. Shang, N. Lu, Y. Wu, Appl. Catal. B-Environ. 184 (2016) 355-363.
[58] W.C. Chung, M.B. Chang, Energy Conv. Manag. 124 (2016) 305-314.
[59] E.C. Neyts, K. Ostrikov, M.K. Sunkara, A. Bogaerts, Chem. Rev. 115 (2015) 13408-13446.
[60] X. Tu, H.J. Gallon, M.V. Twigg, P.A. Gorry, J.C. Whitehead, J. Phys. D-Appl. Phys. 44 (2011) 274007.
[61] L.F. Dong, X.C. Li, Z.Q. Yin, S.F. Qian, J.T. Ouyang, L. Wang, Chinese Phys. Lett. 18 (2001) 1380-1382.
[62] H.H. Kim, A. Ogata, Eur. Phys. J-Appl. Phys. 55 (2011) 13806.
[63] A. Meiners, M. Leck, B. Abel, Rev. Sci. Instrum. 81 (2010) 113507.
[64] B.W. Wang, W.J. Yan, W.J. Ge, X.F. Duan, J. Energy. Chem. 22 (2013) 876-882.
[65] M.S. Lewis-Beck. Applied Regression: An Introduction: SAGE Publications, Inc; 1980.
[66] S.L. Brock, M. Marquez, S.L. Suib, Y. Hayashi, H. Matsumoto, J. Catal. 180 (1998) 225-233.
[67] J.Y. Wang, G.G. Xia, A.M. Huang, S.L. Suib, Y. Hayashi, H. Matsumoto, J. Catal. 185 (1999) 152-159.
[68] R.X. Li, Q. Tang, S. Yin, T. Sato, Plasma Chem. Plasma Process. 26 (2006) 267-276.
[69] R.X. Li, Q. Tang, S. Yin, T. Sato, J. Phys. D-Appl. Phys. 40 (2007) 5187-5191.